npg

PI3K p110α and p110β have differential effects on Akt activation and protection against oxidative stress-induced apoptosis in myoblasts

RW Matheny Jr[1,2] and ML Adamo*[1,2]

Catalytic subunits of phosphoinositide-3-kinase (PI3K) play a critical role in growth factor signaling and survival by phosphorylating inositol lipids. We found that PI3K Class-IA p110α and p110β have distinct functions in myoblasts. Inhibition of p110α reduced insulin-like growth factor-I (IGF-I)-stimulated Akt activity and prevented IGF-I-mediated survival in H_2O_2-treated cells; in contrast, siRNA knockdown of p110β increased IGF-I-stimulated Akt activity. However, inhibition of p110β catalytic activity did not increase IGF-I-stimulated Akt activity, suggesting a role for p110β protein interactions rather than decreased generation of phosphoinositides in this effect. Increased Akt activity in p110β-deficient myoblasts was associated with diminished extracellular signal-regulated kinase (ERK) activation as well as ERK-dependent IRS-1 636/639 phosphorylation, findings we show to be independent of p110β catalytic function, but associated with insulin-like growth factor-I receptor (IGF-IR) endocytosis. We also report that IGF-I protects myoblasts from H_2O_2-induced apoptosis through a mechanism that requires p110α, but may be independent of Akt or ERK under conditions of Akt and ERK inhibition. These observations suggest that both p110α and p110β are essential for growth and metabolism in myoblasts. Overall, our results provide new evidence for the roles of p110 isoforms in promoting cellular proliferation and homeostasis, IGF-IR internalization, and in opposing apoptosis.
Cell Death and Differentiation (2010) **17,** 677–688; doi:10.1038/cdd.2009.150; published online 16 October 2009

Members of the phosphoinositide-3-kinase (PI3K) class of enzymes generate phosphoinositol products that act as second messengers in a number of intracellular signaling cascades.[1] PI3K catalytic enzymes are categorized into three classes by their structure, substrate specificity, and lipid products.[2] Members of the Class-IA PI3Ks (α, β, and δ) are heterodimers consisting of a 110-kDa catalytic subunit and an 85, 55, or 50-kDa regulatory subunit.[2,3] Activation of PI3K leads to proliferation and pro-survival effects; however, dysregulation of PI3K signaling can promote aberrant proliferative signals leading to cellular transformation.[4–7]

Examination of the ubiquitously expressed PI3K Class-IA p110α and p110β catalytic subunits has revealed distinct and redundant roles for each depending on cellular context.[8–10] Heterozygous knock-in of catalytically-inactive p110α or pharmacological inhibition of p110α with a small-molecule inhibitor has been shown to negatively regulate growth, metabolism, and growth factor signaling in mice.[10,11] p110β has been shown to mediate cell growth and development, DNA replication, insulin sensitivity, tumorigenesis, and G-protein-coupled receptor-activated signaling.[12–15] Recently, a kinase-independent, scaffolding role of p110β has been suggested; indeed, this kinase-independent function may play a role in cell proliferation and clatharin-mediated endocytosis.[13,16] Mice doubly heterozygous for p110α and p110β showed mild glucose intolerance and

reduced sensitivity to insulin challenge associated with p85 protein instability, but showed no difference in insulin-stimulated Akt phosphorylation or activity in liver or muscle as compared with control mice.[17]

Insulin-like growth factor-I (IGF-I) is a hormone that promotes proliferation, differentiation, and survival in a number of cells types, mediated principally through PI3K/Akt and Ras/Raf/MEK/ERK pathways.[18–20] IGF-I/PI3K signaling has been shown to promote survival in several apoptosis-inducing models such as serum withdrawal and oxidative stress;[21–23] however, the specific PI3K and Akt isoforms involved in survival are yet to be established. Likewise, PI3K/Akt-independent compensatory survival mechanisms have yet to be fully resolved. We report here that C2C12 myoblasts transfected with siRNA against p110α, p110β, or a combination of both, displayed differential phenotypes with respect to cell growth and PI3K-dependent signaling. Furthermore, we found that IGF-I stimulation differentially regulated Akt phosphorylation and activation in a PI3K and Akt isoform-specific manner, and that p110α was the principal Class-IA PI3K mediating IGF-I antiapoptotic actions. Finally, we report that knockdown p110β negatively regulates insulin-like growth factor-I receptor (IGF-IR) internalization and extracellular signal-regulated kinase (ERK) activation, which was associated with relief of feedback inhibition of PI3K-dependent signal transduction.

[1]Department of Biochemistry, University of Texas Health Science Center at San Antonio, San Antonio, TX 78229, USA and [2]The Sam and Ann Barshop Institute for Longevity and Aging Studies, University of Texas Health Science Center at San Antonio, San Antonio, TX 78229, USA
*Corresponding author: ML Adamo, Department of Biochemistry, University of Texas Health Science Center at San Antonio, MSC 7760, 7703 Floyd Curl Drive, San Antonio, TX 78229-3900, USA. Tel: +210 567 3742; Fax: +120 567 6595; E-mail: adamo@biochem.uthscsa.edu

Results

Reduced cell proliferation in cells treated simultaneously with siRNA against p110α and p110β is associated with increased apoptotic markers, whereas reduced cell proliferation in cells treated with siRNA against p110β alone is not. We first determined that both p110α and p110β are expressed at the mRNA and protein level in C2C12 myoblasts (Figure 1a), but that p110γ and p110δ were not expressed appreciably. In order to establish the efficacy of siRNA-mediated knockdown of p110α and p110β, cells were transfected with siRNA against p110α (si-p110α), p110β (si-p110β), or non-targeting control siRNA (si-Con). Addition of si-p110α resulted in ∼60–65% reduction in p110α mRNA, whereas addition of si-p110β resulted in ∼65% reduction in p110β mRNA (Figure 1b). mRNA levels of p110β were unaffected by p110α knockdown, and mRNA levels of p110α were unaffected by p110β knockdown. To determine whether cell growth was affected by knockdown of p110α, p110β, or the combination (si-p110α + β), cells were counted at 24 and 48 h after transfection. Addition of si-p110β and si-p110α + β caused a reduction in cell number at 48 h for si-p110β ($P < 0.05$) and at 24 and 48 h for si-p110α + β (Figure 1c). This reduction in cell number was associated with increased cleavage of caspase-3 and poly-(ADP)-ribosyl polymerase (PARP), a molecule downstream of caspase-3 and an indicator of apoptosis (Figure 1d).[24] As knockdown of p110α can reduce PI(3,4,5)P3 levels,[11] and p110β may act to maintain basal levels of PI(3,4,5)P3,[10] we analyzed Akt (also known as protein kinase B), an AGC-kinase family member whose activation is known to be regulated by phosphoinositides.[25] Forty-eight hours after transfection, levels of phospho-Akt in the hydrophobic domain (Ser473/ 474/472 in Akt1, Akt2, and Akt3, respectively; hereafter referred to as S473) showed decreased phosphorylation after treatment with p110α; conversely, phospho-Akt Ser 473 levels were increased after treatment with si-p110β alone (Figure 1e). The levels of phosphorylated Akt did not correlate with total p85 levels, as reductions in total p85 were observed in p110α- and p110β-deficient cells, but were
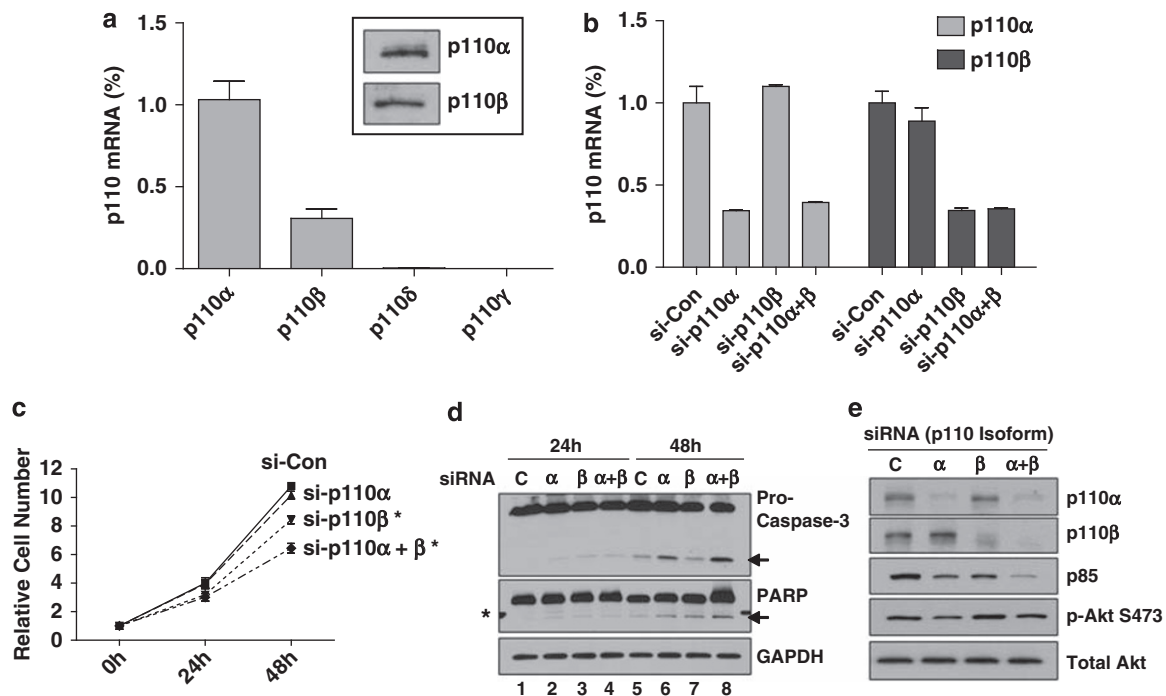

Figure 1 PI3K p110α and p110β are expressed in C2C12 myoblasts and reduction of p110β or p110α and β simultaneously reduced cell growth. (**a**) PI3K p110 catalytic subunit expression in myoblasts. Real-time PCR was used to determine mRNA transcript level as described under Materials and Methods. C_t values were first normalized to invariant endogenous β-2 microglobulin (B2 M), and then values were expressed relative to p110α, which was arbitrarily set at 1.0. Inset: Detection of expressed p110 isoforms by western blotting. (**b**) Efficacy of RNAi-mediated knockdown of p110α and p110β was determined by real-time PCR using B2 M as a reference gene, as in panel **a**. Cells were reverse-transfected with 10 nM negative control siRNA (si-Con) or 5 nM siRNA against p110α (si-p110α) plus 5 nM si-Con, 5 nM p110β (si-p110β) plus 5 nM si-Con, or simultaneous transfection (co-transfection) with 5 nM p110α and 5 nM p110β (si-p110α + β). Medium was changed to antibiotic-containing media 24 h after plating, and cells were harvested for RNA 24 h following media change (48 h after initial reverse transfection). Values are expressed relative to p110α, which was arbitrarily set at 1.0. Columns represent averages of two independent experiments and error bars indicate S.E.M. (**c**) Cells were reverse-transfected as described in panel **b** at day 0. Twenty-four and 48 h after plating, cells were trypsinized and counted with a hemocytometer and expressed as fold changes relative to initial plating density, which was set at 1.0. Asterisks next to treatments indicate significant difference at $P < 0.05$ after two-way ANOVA followed by Bonferroni post-test. (**d**) Cells were transfected as described in panel **b**, and myoblasts were harvested for protein lysates 24 and 48 h after plating. western blotting was performed to analyze levels of caspase-3, PARP, and GAPDH as described under Materials and Methods. Uncleaved caspase-3 and PARP are labeled and cleaved caspase-3 and PARP are indicated by arrows. Numbers 1–8 (bottom) indicate lanes. The asterisk (*) next to the PARP image indicates protein ladder (98 kDa) that reacted with antibody in this and some subsequent runs. Abbreviations: C, non-targeting control siRNA; α, siRNA against p110α; β, siRNA directed against p110β; α + β, siRNA directed against p110α co-transfected with siRNA directed against p110β. (**e**) Cells were treated and maintained as described in panel **b**. Western blots of various proteins involved in PI3K signal transduction are shown. Each blot is representative of two independent experiments. Abbreviations are identical to those described in panel **d**

even further reduced when cells were treated simultaneously with si-p110α and si-p110β (Figure 1e).

RNAi knockdown of p110α reduces, and knockdown of p110β increases, IGF-I-stimulated Akt phosphorylation and activity. As IGF-I can mediate pro-survival effects through Akt, we sought to determine the responsiveness of p110α- and p110β-deficient cells to IGF-I. Addition of IGF-I to cells transfected with si-p110α, si-p110β, or si-p110α + β resulted in increased Akt phosphorylation at the activation loop (Thr308/309/305 in Akt1, Akt2, and Akt3, respectively; hereafter referred to as T308). This increase was reduced in si-p110α-treated cells, but further increased in si-p110β-transfected cells (Figure 2a). IGF-I-stimulated phospho-Akt in cells treated with both si-p110α and p110β together was not statistically lower than si-Con cells treated with IGF-I (Figure 2a). As the sequences surrounding the Akt active site (T308) and hydrophobic motif (S473) residues are similar between isoforms, and because the antibody cannot discriminate between isozymes, we performed *in vitro* kinase assays to determine the relative contributions of each isoform. IGF-I-stimulated Akt1 activity was reduced in cells transfected with si-p110α and si-p110α + β; conversely, Akt1 activity was increased in response to IGF-I in cells treated with si-p110β (Figure 2b). Only cells transfected with si-p110α alone showed reduced Akt3 activity, and there was no increase or decrease in Akt3 activity in cells transfected with either p110β or p110α + β, respectively. Akt2 activity was unchanged by any treatment, and long exposures (shown in Figure 2b) likely represent the background. Taken together, these data suggest that knockdown of p110α reduces IGF-I-stimulated Akt phosphorylation and activation of both Akt1, and Akt3. IGF-I-induced Akt1 activity was greater in si-p110β-transfected cells than IGF-I-stimulated Akt1 activity in control cells, which correlated with increased Akt phosphorylation. Yet, IGF-I-stimulated Akt3 activity did not show this elevation, suggesting that the increase in total Akt phosphorylation may be the result of increased Akt1 activation in p110β-deficient cells. On the other hand, in cells transfected with si-p110α + β, Akt1 activity was diminished, but Akt3 activity was not, suggesting that the increase in IGF-I-stimulated Akt phosphorylation in si-p110α + β-treated cells as compared with si-p110α alone, reflects increased Akt3 activation.

To test whether this increased Akt activity in p110β-knockdown cells correlated with increased p110 association with components of the IGF-IR signaling complex, we performed immunoprecipitation experiments. Treatment of cells with IGF-I promoted p110α and p110β association with insulin receptor substrate-1(IRS-1) and IGF-IR at early time points following administration (Figure 3a, left). In p110α-deficient cells, IGF-I-induced association of both p110α and p110β with IGF-IR and IRS-1 was reduced, whereas in p110β-deficient cells, association of p110α with IGF-IR and IRS-1 was enhanced (Figure 3a, right). Simultaneous knockdown of p110α and p110β prevented IGF-I-induced association of both p110α and p110β with IGF-IR and IRS-1. These findings suggest that IGF-I-induced association of p110α with IGF-IR and IRS-1 is enhanced when p110β levels are reduced. We next determined whether p110α or p110β deficiency affected

IGF-I-stimulated PI(3,4,5)P3 production. IGF-I promoted PI(3,4,5)P3 generation from p110α and p110β immunoprecipitates, and this effect was reduced when cells were deficient in the respective isoform (Figure 3b). Levels of PI(3,4,5)P3 in IGF-I-treated cells transfected with si-p110β were intermediate between unstimulated and IGF-I-stimulated control cells. Altogether, these data suggest that Akt activation correlates with levels of the p110–IGF-IR complex, but in cells deficient in p110β, mechanisms other than PI(3,4,5)P3 production may contribute to elevated Akt activation.

Knockdown of p110β is associated with decreased ERK signaling and IGF-IR internalization. To further elucidate the mechanism whereby Akt phosphorylation and activity is increased in p110β-deficient cells, as well as to further characterize intracellular responses to p110 catalytic subunit deficiency, we examined other molecules involved in canonical IGF-I signaling pathway. In cells deficient in p110β alone, or deficient in p110α and p110β, we found that phosphorylation of ERK was reduced in the basal state as well as after stimulation with IGF-I (Figure 4a). Additionally, IGF-I-stimulated phosphorylation of IRS-1 at Ser 636/639 was attenuated under conditions of reduced p110β, a finding consistent with previous work suggesting dependence on ERK for IRS serine phosphorylation at this site.[26]

To determine whether decreased ERK phosphorylation seen in p110β-deficient cells was due to an overall decrease in p110β protein levels or due to decreased catalytic activity, cells were treated with increasing concentrations of TGX-221, an inhibitor of p110β catalytic function. Addition of TGX-221 reduced LPA-induced Akt phosphorylation in a dose-dependent manner, but did not affect IGF-I-stimulated ERK phosphorylation at any concentration tested (Figure 4b). These data suggest that the decreased levels of phosphorylated ERK observed in p110β-deficient cells may result from a loss of total p110β rather than loss of catalytic function, a finding consistent with a scaffolding action of p110β.

To address whether this catalysis-independent function of p110β mediates IGF-IR internalization, we examined the presence of IGF-IR at the cell surface after IGF-I treatment in the absence or presence of TGX-221 or si-p110β. Treatment of myoblasts with IGF-I resulted in a reduction in cell-surface IGF-IR that was maximal after 30 min (Figure 4c, left). In IGF-I-stimulated cells pretreated with 100 nM TGX-221, IGF-IR internalization was similar to IGF-I treatment alone; however, in cells deficient in p110β, IGF-IR did not internalize in response to IGF-I (Figure 4c, right). These findings suggest that at least one kinase-independent role of p110β in myoblasts is to mediate IGF-IR internalization.

IGF-I acts through PI3K p110α to prevent H$_2$O$_2$-induced apoptosis. To establish whether the differential signaling effects of p110α and p110β knockdown extend to physiological actions in a proapoptotic milieu, cells were examined to determine whether knockdown of p110 isoforms was sufficient to inhibit IGF-I from preventing oxidative stress-induced cell death. To first test this, we employed an inhibitor specific to PI3K p110α (p110αi),[27] since broad-spectrum PI3K pharmacological inhibitors, such as
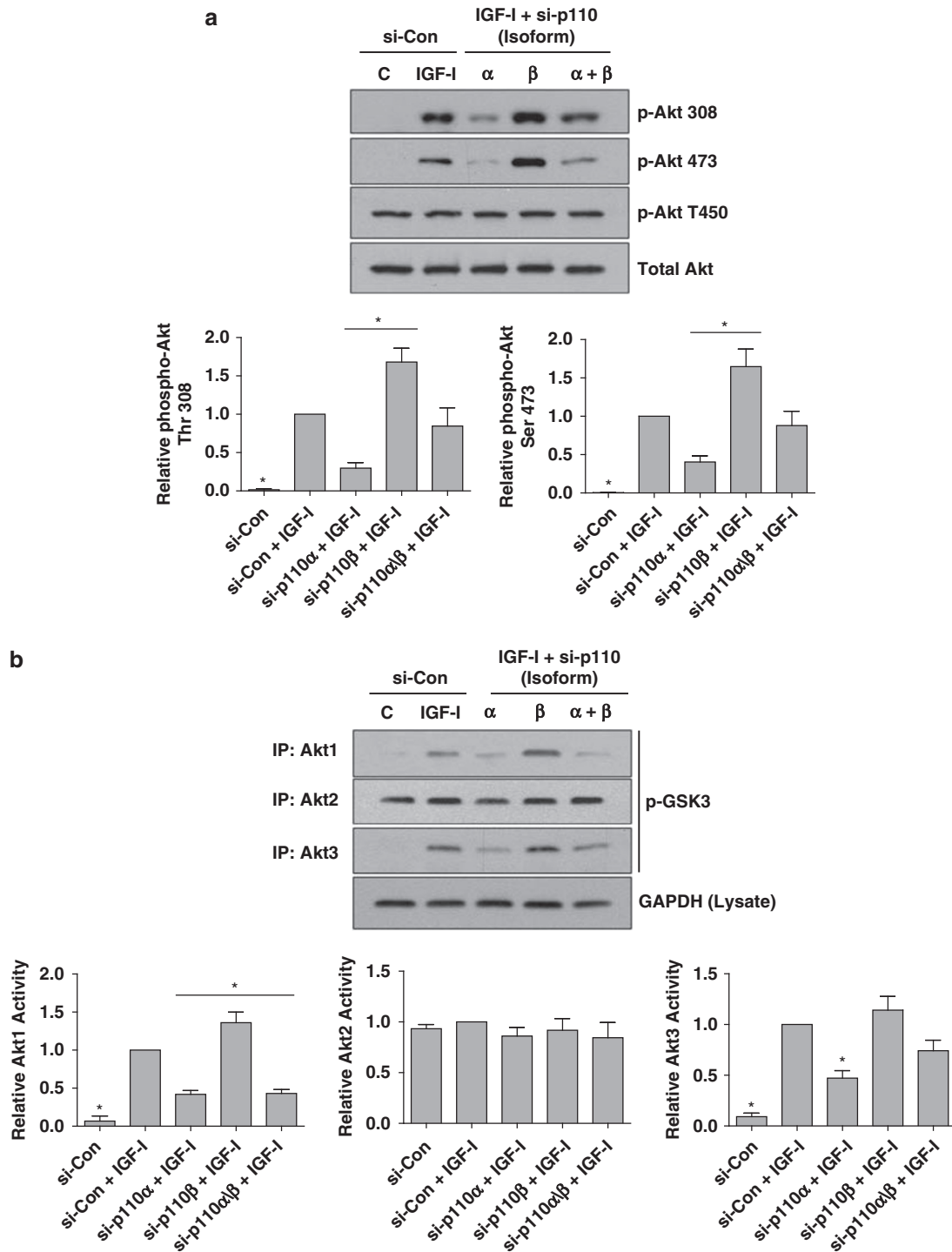
Figure 2 RNAi-mediated knockdown of p110α reduces Akt phosphorylation at Thr 308 and Ser 473 and activation of Akt1 and Akt3, while p110β knockdown does not. (**a**) Cells were reverse-transfected and maintained as described in Figure 1b. Forty-eight hours after transfection, cells were treated with 125 ng/ml IGF-I for 30 min and then harvested for protein lysates, upon which western blotting was performed using the antibody indicated to the right of the images. Levels of phosphorylated Akt were normalized to total Akt for each specific run, and the level of IGF-I-stimulated Akt phosphorylation was set to 1.0. Quantification was performed using Image J software (http://rsbweb.nih.gov/ij/) as described in Materials and Methods. Columns in graphs represent the averages of 3–5 independent experiments, and error bars represent S.E.M. Asterisks indicate significant difference from IGF-I-stimulated values ($P < 0.05$; one-way ANOVA followed by Dunnett's multiple comparisons test), and horizontal bars directly below the asterisks span columns statistically different from IGF-I-stimulated values. (**b**) Activities of Akt isoforms were measured by *in vitro* kinase assay (IVK) as described in Materials and Methods. The antibody used for immunoprecipitation is indicated to the right, and experiments were performed 3–5 times. Levels of GAPDH were determined by western blotting on protein lysates. Isoform-specific activated Akt levels were normalized to GAPDH for each specific run, and the level of IGF-I-stimulated Akt phosphorylation was set to 1.0. Columns in the graphs represent the averages of 3–5 independent experiments, and error bars represent S.E.M. Significant differences were determined as described in (**a**)
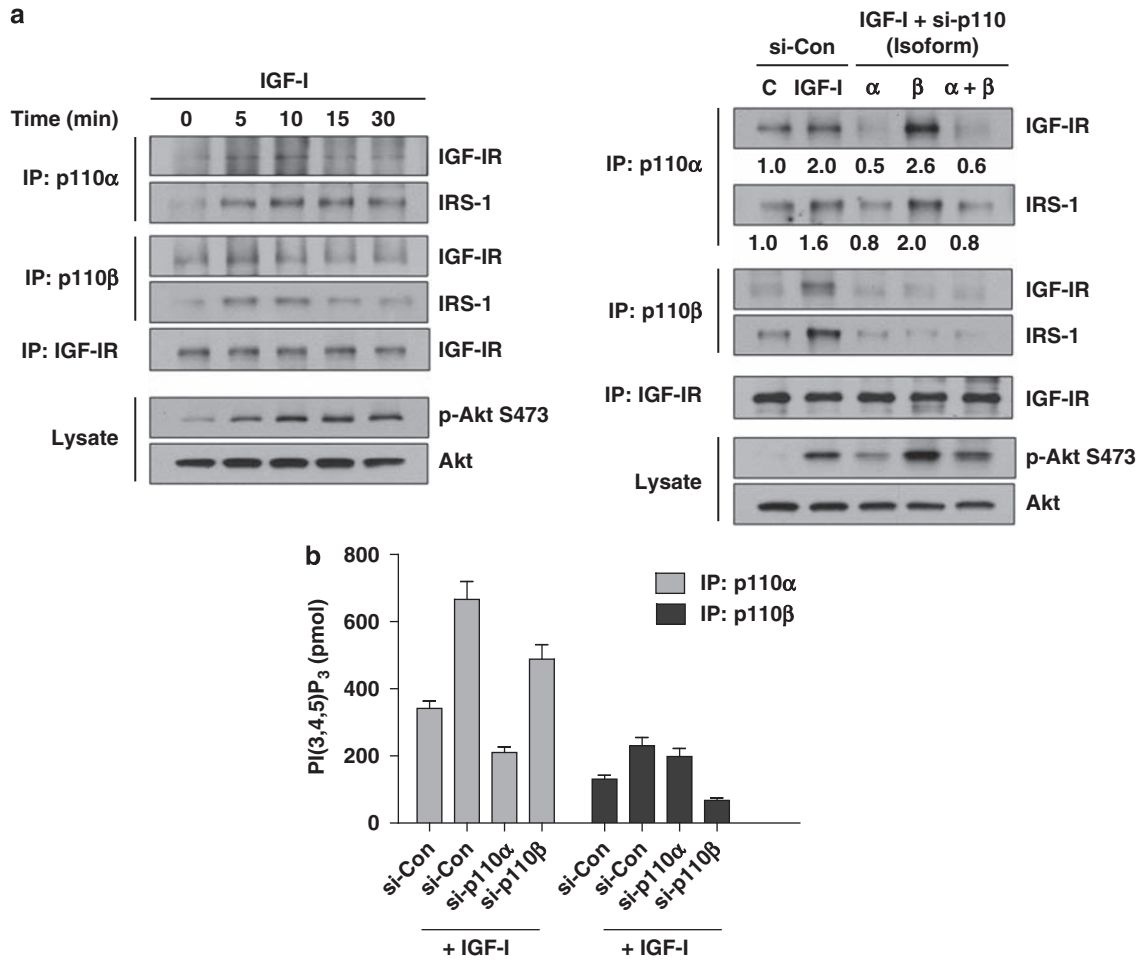
Figure 3 IGF-I effects on p110 subunit association with IGF-IR signaling complex and PI(3,4,5)P3 generation. (**a**) Left: Cells were treated with 125 ng/ml IGF-I and then harvested at the indicated times. Immunoprecipitation (IP) with antibodies against p110α, p110β, or IGF-IR is indicated at the left of the images. Western blotting using the primary antibodies noted to the right of the images was performed as described under Materials and Methods. For phospho-Akt and total Akt, western blotting was performed without IP (lysate). Right: Cells were treated with 125 ng/ml IGF-I for 7 min before harvesting. IP and western blotting were performed as described directly above. Numbers below blots indicate band density as compared with unstimulated control cells, which was set at 1.0. Shown are representative results from three independent experiments. (**b**) Cells were reverse-transfected as described in Figure 1b. Forty-eight hours after transfection, cells with were treated with 125 ng/ml IGF-I and then harvested after 7 min. IPs were performed on 125 μg cell lysate using antibodies against p110α or p110β, followed by kinase reactions and detection of PI(3,4,5)P3 levels by ELISA as described under Materials and Methods. Data represent means of triplicate experiments, and error bars indicate SD

LY294002 and wortmannin, do not discriminate between isoforms. Caspase-3 and PARP cleavage was increased in cells treated with 400 μM H_2O_2 for 4 h, an effect that was completely prevented by a 30-min pretreatment with IGF-I (Figure 5a and b, lanes 1–4). Caspase-3 and PARP cleavage was increased in p110αi and p110αi + H_2O_2-treated cells, and p110αi completely prevented IGF-I from inhibiting apoptosis (Figure 5a and b, lanes 7–8; compare with lanes 1–2). In contrast, treatment of myoblasts with IGF-I in the presence of the p110β inhibitor TGX-221 did not prevent IGF-I from reducing H_2O_2-stimulated caspase-3 and PARP cleavage (Figure 5c, right).

To confirm these results, we employed siRNA directed against p110α and p110β. Cells were pretreated with IGF-I, treated with H_2O_2, or both in the presence or absence of si-p110α, si-p110β, or si-p110α + β. Similar to the inhibitor results, IGF-I was unable to prevent H_2O_2-induced cleavage of caspase-3 and PARP in cells deficient in p110α whether

transfected with si-p110α alone (Figure 5d, left) or in combination with si-p110β (Figure 5d, right). Cells pretreated with si-p110β appeared partially resistant to H_2O_2-induced apoptosis (Figure 5d, middle), possibly a result of increased Akt activation (Figure 2). Taken together, these data suggest that IGF-I acts through PI3-K p110α isoform to prevent H_2O_2-induced apoptosis in myoblasts exposed to oxidative stress.

Since reduction of p110β effectively inhibited phosphory-lated ERK levels while simultaneously increasing Akt activation, we next tested whether Akt was a primary survival intermediate in p110β-knockdown cells. Maximal inhibition of IGF-I-stimulated phosphorylation of Akt S473 was obtained at a concentration of 10 μM using a compound specific for Akt (Akti; reference Barnett et al.;[28] Figure 5e, left). IGF-I was unable to prevent H_2O_2-induced apoptosis in p110β-trans-fected cells (Figure 5e, right) also treated with Akti, thus confirming that a functional Akt pathway is necessary for survival in p110β-deficient myoblasts.
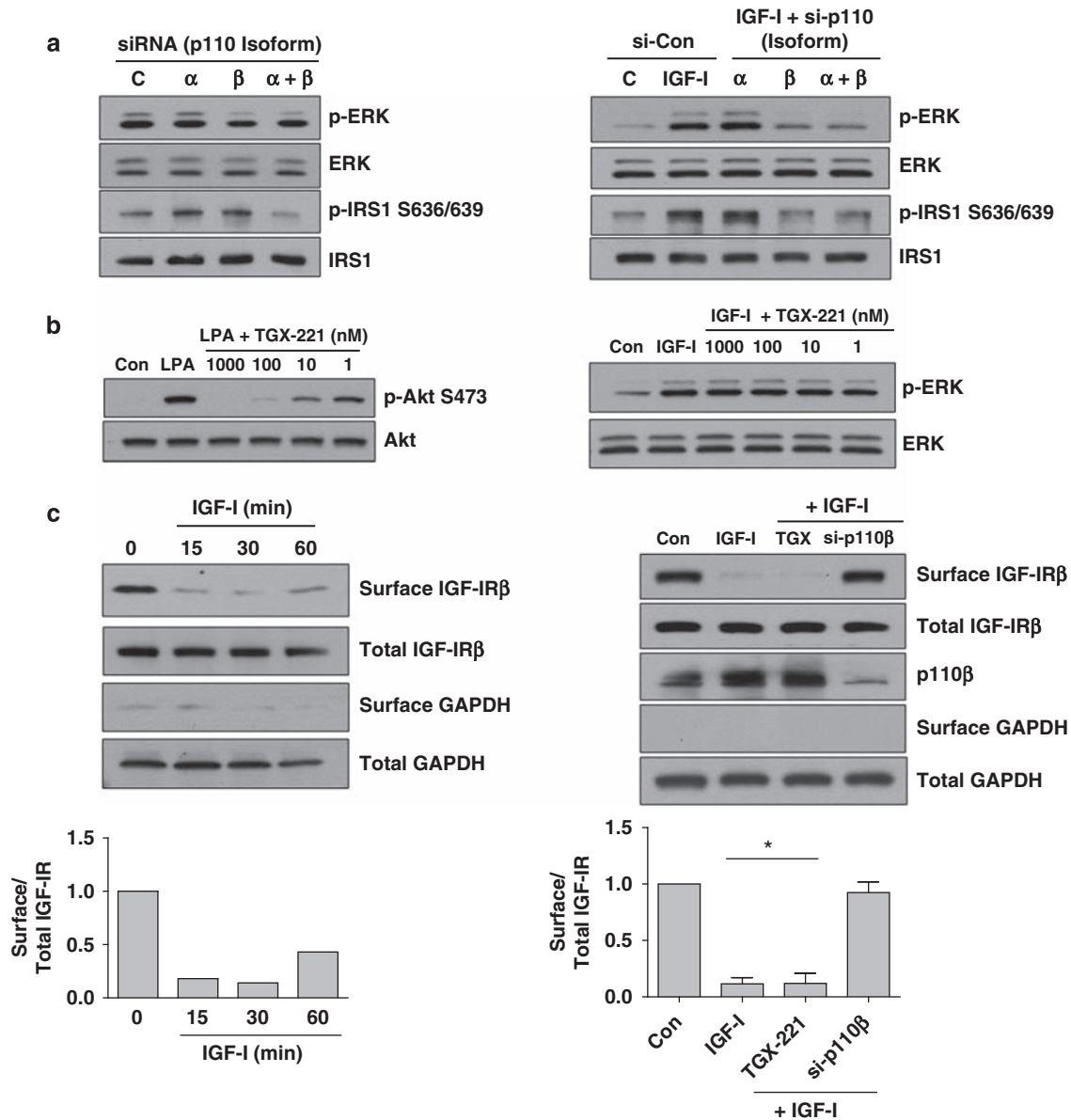
Figure 4 p110β knockdown, but not catalytic inhibition, reduces IGF-I-mediated ERK phosphorylation and IGF-IR internalization. (**a**) Cells were reverse-transfected and maintained as described in Figure 1b. Forty-eight hours after transfection, cells were harvested or treated with 125 ng/ml IGF-I for 30 min and then harvested for protein lysates. Western blotting was performed using antibodies indicated to the right of the respective images. Blots are representative of two independent experiments. (**b**) 95% confluent C2C12 myoblasts were pretreated with TGX-221 at the indicated concentrations for 1 h before addition of 20 μM LPA or 125 ng/ml IGF-I for 30 min. Western blots using the antibody against the indicated protein were then performed. (**c**) Quantity of IGF-IR at the cell surface after IGF-I administration was determined by biotin labeling and immunoprecipitation of surface proteins. Left panel: Cells were treated with 125 ng/ml IGF-I for the indicated times, labeled with sulfo-NHS-SS-biotin, and isolated according to the procedure described under Materials and Methods. The amount of IGF-IR located at the cell surface determined by western blotting after immunoprecipitation with NeutrAvidin Agarose; levels of total IGF-IR and GAPDH were determined by analyzing total cell lysate prior to immunoprecipitation. Columns represent quantified levels of surface IGF-IR divided by total IGF-IR normalized to untreated control, which was set at 1.0. Right panel: Cells were treated with 125 ng/ml IGF-I for 30 min after pretreatment with negative control siRNA (unlabeled) for 48 h, si-Con for 48 h, and TGX-221 for 1 h ('TGX-221'), or 5 nM siRNA against p110β ('si-p110β') for 48 h. Surface and total levels of indicated proteins were determined as described above. Columns represent quantified levels of surface IGF-IR divided by total IGF-IR from two independent experiments normalized to untreated control, which was set at 1.0. Asterisk indicates significant difference from unstimulated cells as determined by ANOVA with Tukey's HSD test *post hoc* ($P < 0.05$). Error bars represent SD

IGF-I acts through alternative signaling pathways to prevent apoptosis induced by deficiency of p110α alone, by p110α + p110β, or by H₂O₂. We noted that knockdown of p110α or p110α + β increased caspase-3 and PARP cleavage (lanes 1–2 compared with lanes 5–6; Figure 5a, b, and d), an effect that was reversed by IGF-I administration. To determine

the identity of pathway(s) or molecule(s) involved in this effect, cells were treated with an inhibitor of Akt (Akti) or of mitogen-activated ERK kinase (MEK) (U0126). Cells were pre-incubated with inhibitors of increasing concentrations for 1 h, and then exposed to IGF-I for 4.5 h. A 10-μM U0126 concentration completely prevented IGF-I-stimulated

phosphorylation of p42/p44 ERK at 30 min, and 4.5 h after IGF-I administration, levels of phospho-ERK remained slightly below that of IGF-I-naive cells (Figure 6a, left). Cells treated with si-p110α or si-p110α + β were pre-incubated with either Akti or U0126 and then stimulated with IGF-I for 4.5 h. Pharmacological blockade of MEK in IGF-I-treated p110α-deficient cells prevented IGF-I-induced survival, and blockade of Akt increased p110α-deficiency-induced apoptosis beyond that of the MEK inhibitor (Figure 6a, right). However, in p110α + p110β-deficient cells, inhibition of Akt, but not MEK, fully prevented IGF-I pro-survival signaling. These data suggest that when p110α, and by extension Akt activation, is reduced, IGF-I survival signaling compensates by increased flux through the MAPK pathway. On the other hand, when cells are deficient in both p110α and p110β, IGF-I signals primarily through Akt to promote survival.

As IGF-I differentially acts through Akt and MEK pathways to promote survival from p110α and p110α + p110β-deficiency-induced apoptosis, we sought to determine whether these pathways were also involved in preventing H_2O_2-induced apoptosis. Blockade of Akt, ERK, or concurrent inhibition of both, did not prevent IGF-I from inhibiting caspase-3 or PARP cleavage (Figure 6b). These data suggest that, although Akt and ERK pathways can compensate for each other in response to IGF-I, at least one more mechanism exist through which IGF-I can exert antiapoptotic effects in response to oxidative stress in myoblasts.

Discussion

In this work, we report that myoblasts deficient in p110α and/or p110β show disparate growth and intracellular signaling phenotypes, corresponding with differential regulation of Akt and ERK signaling pathways. One key observation was that knockdown of p110α inhibited, but knockdown of p110β promoted, the activation of Akt in an isoform-specific manner. Although p110β may play a secondary role in growth factor signaling by maintaining a basal pool of PI (3, 4, 5)P3,[10,13] it is not generally thought to play a primary role in RTK-instigated signaling except under certain conditions such as PTEN loss, or in certain cell types.[2,29] Our results suggest that p110β deficiency leads to increased Akt activation through two separate mechanisms: First, reduced p110β levels enhance the IGF-I-induced association of p110α with IGF-IR and IRS-1. Second, reduced p110β levels inhibit phosphorylation of ERK and IRS-1 at S636/639, thereby relieving IRS-associated negative feedback. One intriguing finding was that increased IGF-I-stimulated Akt activation in p110β-deficient cells did not correlate with increased PI(3,4,5)P3 production, a finding consistent with previous results using skeletal muscle of insulin-stimulated $p110\alpha^{+/-}/p110\beta^{+/-}$ mice.[17] Those authors suggested that decreased p85 levels may contribute to insulin sensitivity, and indeed, in our study we observed lowered p85 in p110β-deficient cells (Figure 1e).

Furthermore, our finding that serine phosphorylation of IRS-1 at Serine 636/639, a site dependent on ERK,[26] is reduced, is consistent with a relief of negative PI3K-signaling feedback.[30] Since IGF-I-stimulated Akt activity did not statistically differ between control and p110α + p110β-deficient cells (Figure 2b), yet there being virtually no p110/IGF-IR/IRS-1

association (Figure 2c, right), the loss of feedback inhibition in p110α + p110β-deficient myoblasts may explain the mechanism underlying the similarity in Akt activation. Indeed, in skeletal muscle of insulin-stimulated $p110\alpha^{+/-}/p110\beta^{+/-}$ mice, Akt phosphorylation was similar to that observed in muscle of insulin-treated, wild-type mice. It is possible that other mechanism(s) contribute to increased Akt activation in p110β-deficient cells, including decreased actions of Akt-specific phosphatases,[31,32] but whether activation of these phosphatases is reduced under these conditions remains to be investigated. Altogether, our observations suggest that increased IGF-I-stimulated Akt activity in p110β-deficient myoblasts may result from both an increase in p110α/IRS-1/IGF-IR association as well as decreased negative feedback to IRS-1 secondary to reduced ERK activation. That distinct Akt isoforms are differentially regulated suggests a high degree of fine-tuning in these processes. Figure 7 presents this signaling model diagrammatically.

The lower levels of ERK phosphorylation in p110β-deficient cells may be reflective of decreased association of p110β with Ras, an upstream molecule in the MAPK signaling pathway; indeed, ERK activation has been shown to be attenuated under conditions where p110β cannot bind to Ras.[4,5] However, use of TGX-221, a compound that inhibits p110β catalytic activity, did not prevent ERK phosphorylation in response to IGF-I in this study. These results suggest that non-catalytic functions of p110β may be essential for ERK activation in myoblasts; in support of this, cells deficient in p110β also showed decreased IGF-IR internalization in addition to attenuated ERK signaling. This is in agreement with previous work suggesting requirement for IGF-IR internalization for activation of upstream MAPK pathway components in CHO cells;[33] additionally, p110β itself has been shown to modulate EGFR and transferrin uptake.[13,16] Taken together, these data and ours support the hypothesis of a kinase-independent function of p110β in IGF-IR internalization and signaling. Consequently, p110β may play a role in IGF-I-mediated processes in skeletal muscle such as progenitor cell proliferation, survival, and differentiation, which occur during muscle development and repair/regeneration.

In light of the above findings, it was not surprising that inhibition of p110α by means of pharmacological blockade or siRNA completely prevented IGF-I from reducing caspase-3 and PARP cleavage in response to H_2O_2, whereas TGX-221- or RNAi-induced silencing of p110β did not (Figure 5a–d). Akt is a critical mediator of antiapoptotic signaling, acting to suppress apoptosis by phosphorylation and inactivation of proapoptotic molecules such as apoptosis-signal-regulating kinase-1 (Ask1),[34] Bad,[35] and FoxO3a.[36] As Akt signaling was reduced after p110α knockdown or treatment with p110αi, it would logically follow that suppression of Akt-targeted proapoptotic molecules would also be attenuated. Likewise, because Akt activation was elevated with p110β knockdown, and this was found to be necessary for survival, IGF-I-stimulated Akt actions would also be elevated.

Myoblasts deficient in p110α or p110α and p110β together showed increased caspase-3 and PARP cleavage, an effect fully reversed by IGF-I. We found that inhibition of MEK prevented IGF-I from attenuating p110α-deficiency-induced caspase-3 and PARP cleavage, and that inhibition of Akt

caused apoptosis in excess of p110α deficiency alone. Inhibition of Akt, but not MEK, prevented IGF-I from attenuating p110α + p110β-deficiency-induced caspase-3 and PARP cleavage (Figure 6a). These data suggest that IGF-I can act through an MEK-dependent pathway to rescue cells from apoptosis associated with p110α deficiency, but that myoblasts under these conditions are more sensitive to loss of Akt, possibly resulting from the reduced Akt activation associated with p110α deficiency. Likewise, in cells simultaneously deficient in p110α and p110β, blockade of Akt prevented IGF-I from opposing apoptosis, whereas blockade of MEK had minimal effects. This is consistent with our findings that ERK activation is inherently reduced under

conditions of p110β deficiency, whether alone or in combination with p110α reduction.

We found that IGF-I was still able to prevent H_2O_2-induced apoptosis even under conditions of Akt and MEK blockade. However, our results also suggest a dependence on p110α. Therefore, our data collectively suggest that IGF-I is capable of preventing H_2O_2-induced apoptosis through an Akt- and MEK-independent, but p110α-dependent, mechanism. Since other AGC kinases are also regulated through p110α in response to IGF-I, it is possible that one or several may contribute to opposing apoptosis. For example, serum- and glucocorticoid-inducible kinase-1 (SGK1) can phosphorylate and inhibit proapoptotic FoxO3a at the same sites as Akt,
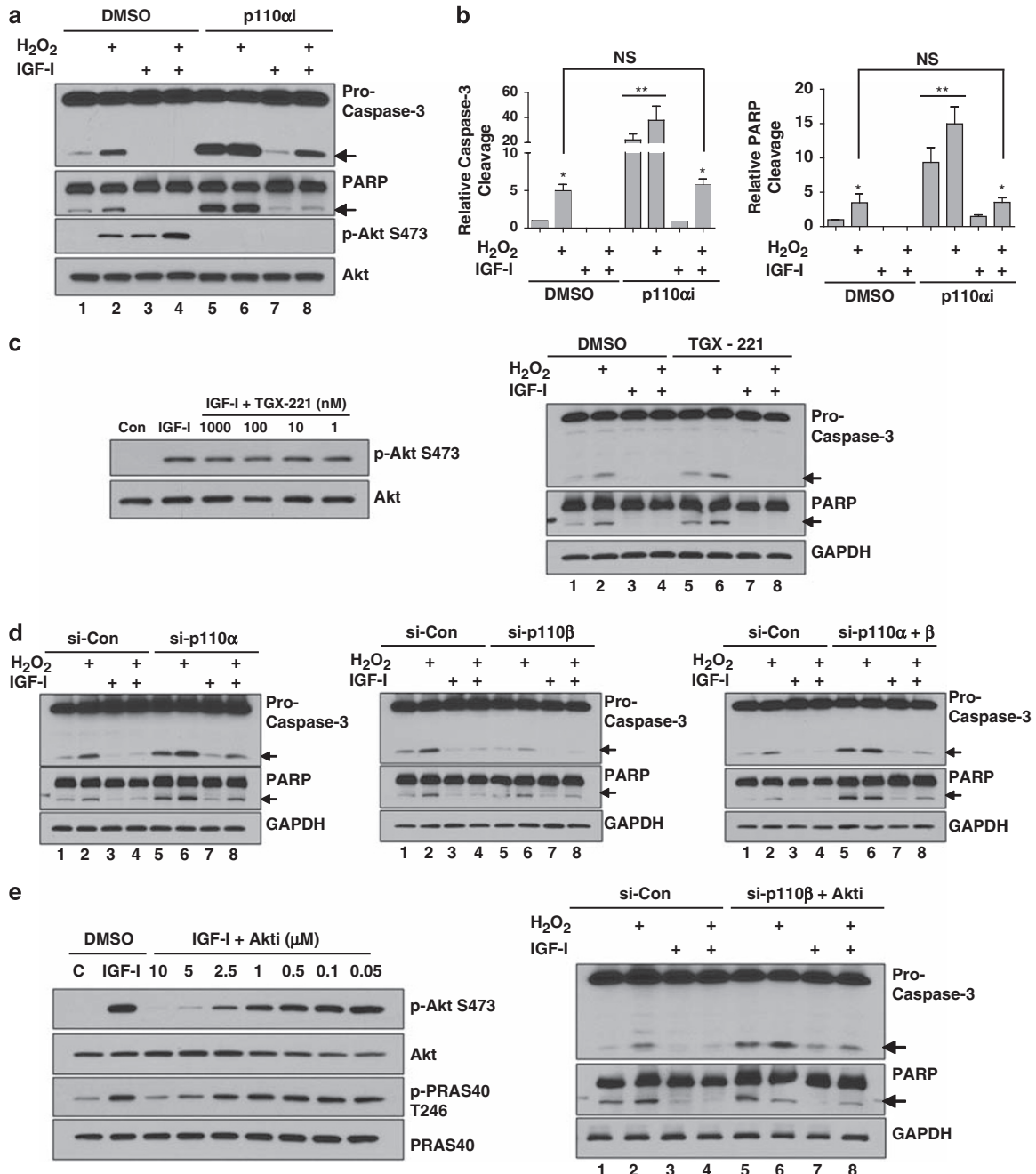
although there exists a preference for some sites over others.[37]

In conclusion, we found that knockdown of p110α and p110β have differential effects on cell growth, survival signaling, and Akt activation. We have defined a kinase-independent role for p110β in IGF-IR internalization and ERK phosphorylation, which is associated with negative feedback to the IGF-IR/IRS-1 signaling complex. Additionally, we identified p110α as the primary Class-IA PI3K involved in IGF-I-mediated rescue from oxidative stress-induced apoptosis and that, in the absence of Akt and MEK-dependent signaling, IGF-I can still prevent H_2O_2-induced apoptosis, but through a mechanism that requires p110α.

Materials and Methods

Materials. C2C12 murine myoblasts were purchased from ATCC (Manassas, VA, USA). H_2O_2 and bovine serum albumin (fraction V) was purchased from Sigma (St Loius, MO, USA). rhIGF-I was purchased form Austral Biologicals (San Ramon, CA, USA). Primary antibodies directed against p110β and GAPDH, and HRP-linked secondary antibodies were purchased from Santa Cruz (Santa Cruz, CA, USA); all other antibodies were obtained from Cell Signaling Technologies (Danvers, MA, USA). PI3Kα inhibitor-IV ('p110αi' in this paper, corresponds to Figure 15e in reference Hayakawa et al.[27]), TGX-221, Akt 1/2 inhibitor VIII ('Akti'), and U0126 were purchased from Calbiochem (San Diego, CA, USA). LPA (18 : 1 oleoyl) was purchased from Avanti Polar Lipids (Alabaster, AL, USA).

Cell culture conditions and siRNA transfections. C2C12 myoblasts were maintained in high-glucose DMEM containing 10% FBS and antibiotics (growth medium), with medium being replenished after 24 h. Forty-eight hours after initial seeding cells were ∼95% confluent and unless otherwise indicated, experiments were conducted under these conditions (in growth medium). Pre-designed Silencer Select siRNAs for mouse p110α (ID no. s71604), p110β (ID no. s93108), and negative controls (non-targeting siRNA, ID no. 4390843) were purchased from Ambion Inc. (Austin, TX, USA). Cells (1.8×10^5/well in six-well culture dish) were reverse-transfected with double-stranded siRNA in antibiotic-free DMEM plus 10% FBS using Lipofectamine 2000 according to manufacturer's instructions (Invitrogen, Carlsbad, CA, USA). Twenty-four hours after reverse transfection, medium was changed to DMEM with 10% FBS containing antibiotics. RNA was isolated 48 h after transfections using RNA-STAT (Tel-test, Friendswood, TX, USA), quantified, and the level of silencing quantitated by real-time PCR as described later in this section. In some cases, protein was isolated 48 h after transfection and the level of silencing determined by western blotting.

Cell counts. Medium was removed from plates and monolayers detached with 0.05% trypsin–EDTA (Gibco, Carlsbad, CA, USA). Cells were suspended in growth medium and counted in a hemacytometer chamber.

RNA Isolation, cDNA synthesis, and real-time PCR. Conversion of total RNA to single-stranded cDNA was accomplished using the High-Capacity cDNA Archive kit (P/N 4322171; Applied Biosystems, Foster City, CA, USA). Briefly, 2 μg total RNA was reverse transcribed using random primers for the following incubation times: 25°C for 10 min, then 37°C for 2 h. cDNA samples were stored at −80°C until use. TaqMan-MGB p110α (Mm00435673_m1), p110β (Mm00659576_m1), p110γ (Mm00445038_m1), p110δ (Mm00435674_m1), and B2M (Mm00437762_m1) probe and primers were purchased from Applied Biosystems as 'Gene Expression Assays.' Real-time PCR reaction was performed within an ABI 7500 thermal cycler. The fluorescence of 3–15 cycles was set up as background. Data were collected at the annealing step of each cycle, and the threshold cycle (C_t) for each sample was calculated by determining the point at which the fluorescence exceeded the threshold limit. The standard curve was generated automatically using a software by plotting the C_t values against each standard of known concentration and calculation of the linear regression line of this curve. Serially diluted amounts of RNA were used to establish standard curves. All samples were run in duplicate.

Protein extraction, immunoprecipitation, and Western Immunoblotting. C2C12 cells were harvested in ice-cold lysis buffer (20 mM Tris-HCl (pH 7.5), 150 mM NaCl, 1 mM Na_2EDTA, 1 mM EGTA, 1% Triton, 2.5 mM sodium pyrophosphate, 1 mM β-glycerophosphate, 1 mM Na_3VO_4, 1 μg/ml leupeptin, 1 mM PMSF, and 1 : 100 dilution of phosphatase inhibitor cocktails 1 and 2 (Sigma)). Homogenates were triturated through a small-bore needle, incubated on ice for 30 min, and centrifuged at $14\,000 \times g$ for 10 min at 4 °C. Protein concentrations were determined by Bradford method.[38] For immunoprecipitations, 200 μg of protein lysate were co-incubated with 4 μl of respective antibody in 200 μl cell lysis buffer with gentle rotation overnight at 4 °C. A 20-μl of Protein-A/G agarose slurry (Santa Cruz) was then added and rotated an additional 2–4 h at 4°C. Complexes were centrifuged at $14\,000 \times g$ and washed five times in wash buffer before addition of 20 μl 2 × Laemmli buffer and then boiled for 5 min. For western blotting, equal amounts of cell lysate proteins (typically 25 μg) were electrophoresed through denaturing SDS-PAGE. Proteins were transferred to PVDF membranes (Millipore Corp., Bedford, MA, USA). Membranes were incubated for 1 h in 5% dry milk solution in Tris-buffered saline plus 0.5% Tween-20 (TBST) and then incubated with the appropriate primary antibody at an appropriate dilution overnight in 5% BSA in TBST. Membranes were washed three times in TBST followed by incubation with the appropriate secondary antibody and again washed three times. Membranes were incubated with enhanced chemiluminescence reagents (Thermo Fisher, Rockford, IL, USA) and exposed to film.

Figure 5 p110α is necessary for IGF-I-mediated protection from H_2O_2-induced apoptosis. (**a**) Approximately 95% confluent myoblasts were treated with 125 ng/ml IGF-I for 30 min in the indicated lanes. Some cells were then treated for an additional 4 h with 400 μM H_2O_2, as indicated. For cells treated with p110α inhibitor (p110αi), cells were pretreated for an additional hour prior to IGF-I, H_2O_2, or IGF-I + H_2O_2 addition. Control cells were treated with DMSO (p110αi diluent) and/or water (H_2O_2 and IGF-I diluent), as appropriate. Four hours after H_2O_2 addition, cells were harvested and western blots performed to detect levels of caspase-3, PARP, phospho-Akt Ser 473, or total Akt (cleaved caspase-3: −17 kDa, cleaved PARP: −85 kDa). Numbers 1–8 along the bottom of the western blots indicate lane numbers. Blots are representative of 3–5 independent experiments. (**b**) Amounts of cleaved caspase-3 and PARP were quantified. Due to heteroscedasticity, values were transformed as $y = -1 * \log(y)$, and significant differences determined by one-way ANOVA followed by Bonferroni post hoc test. Values are expressed relative to unstimulated controls, and the original, non-transformed data is shown. Asterisks indicate significant difference from control, and double asterisks indicate significant differences from control and H_2O_2-treated cells. Horizontal bars directly below asterisks span columns statistically different from control and H_2O_2-treated cells. NS, not significant. (**c**) Left panel: Approximately 95% confluent myoblasts were pretreated with DMSO (unlabeled) or TGX-221 for 1 h before addition of IGF-I for 30 min. Western blots were performed using the indicated antibodies. Right panel: Cells were treated with IGF-I, H_2O_2, or TGX-221 in place of p110αi exactly as described in panel **a**. (**d**) Cells were reverse-transfected with 5 nM negative control siRNA (si-Con) or 5 nM siRNA against p110α (si-p110α; left panel), 5 nM si-Con or 5 nM p110β (si-p110β; middle panel), or 10 nM si-Con or 5 nM p110α and 5 nM p110β (si-p110α + β; right panel). Forty-eight hours after transfection, myoblasts were treated with 125 ng/ml IGF-I for 30 min in the indicated lanes. Some cells were then treated for an additional 4 h with 400 μM H_2O_2, as indicated. Controls for IGF-I and H_2O_2 were water. Western blotting was performed and the levels of caspase-3, PARP, and GAPDH (as a loading control) analyzed. Intact caspase-3 and PARP are labeled and cleaved portions are indicated by the arrow (cleaved caspase-3: −17 kDa, cleaved PARP: −85 kDa). Numbers 1–8 along the bottom of images represent lane numbers. Blots are representative of three independent experiments. (**e**) Left panel: Approximately 95% confluent myoblasts were pretreated with 0.1% DMSO or increasing concentrations of Akti for 1 h before addition of IGF-I for 4.5 h. Western blotting was performed using the indicated antibodies. Right panel: Cells were reverse-transfected with siRNA against p110β as described above in panel **d**. Forty-eight hours following transfection, some cells were pre-incubated with 10 μM Akti. Following the 1 h incubation period, cells were treated with 400 μM H_2O_2 for 4 h before harvest and western blotting with the indicated antibodies. Blots are representative of two independent experiments
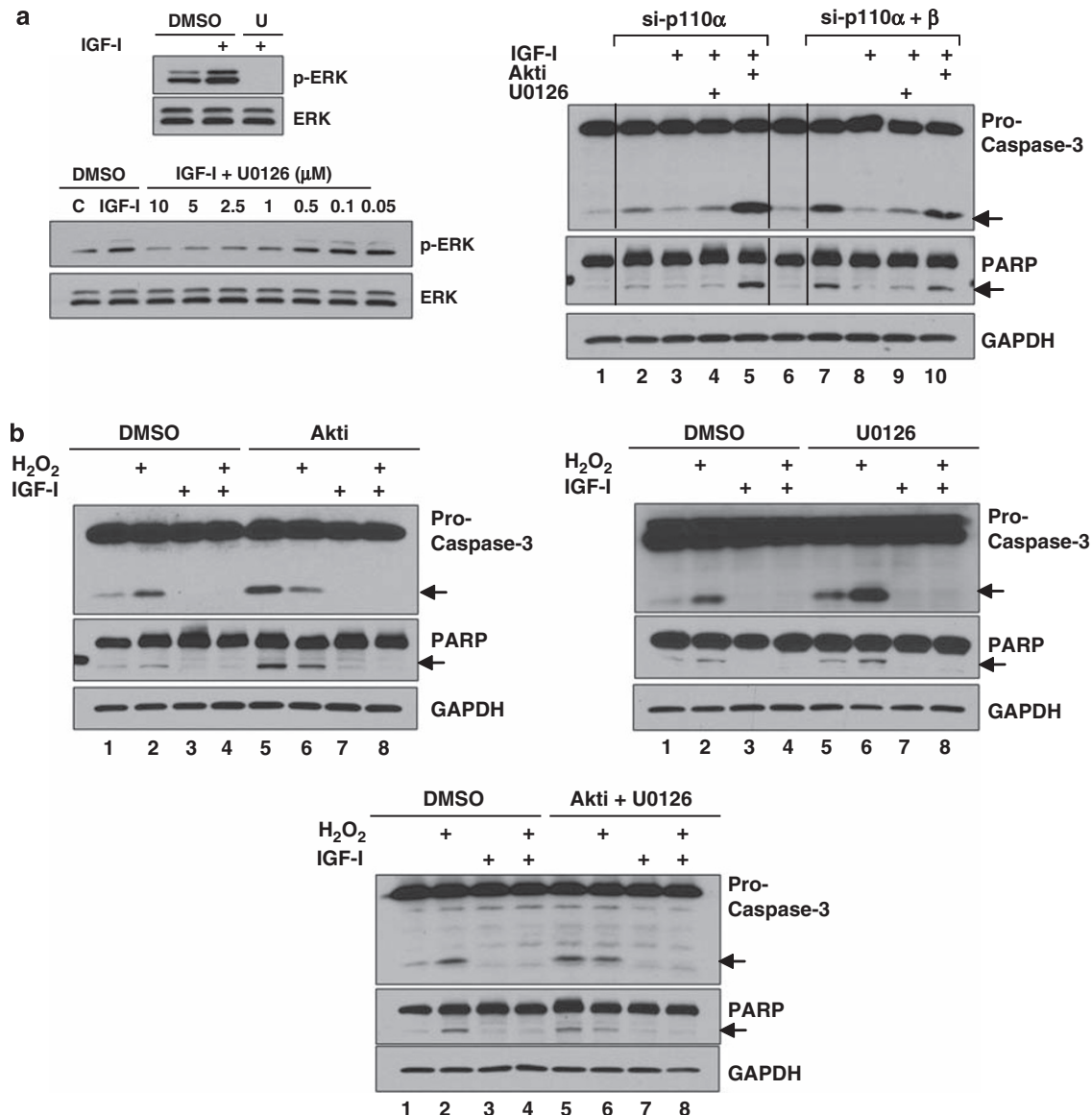
Figure 6 Pharmacological inhibition of Akt and MEK. (**a**) Upper panel: Cells were pre-incubated with 10 μM MEK inhibitor U0126 or 0.1% DMSO for 1 h and then treated with 125 ng/ml IGF-I for 30 min. Levels of phospho- and total ERK were analyzed by western blotting. Lower panel: Cells were pre-incubated with increasing concentrations of U0126 or 0.1% DMSO for 1 h and then treated with 125 ng/ml IGF-I for 4.5 h. Levels of phospho- and total ERK were analyzed by western blotting. 'C': IGF-I control cells treated with water. Right panel: Cells were reverse-transfected and maintained as described in Figure 1b. Myoblasts were pretreated with Akti or U0126 for 1 h as indicated. Following the pre-incubation period, cells were treated with 125 ng/ml IGF-I for 4 h in the indicated lanes. Western blotting was performed and the levels of caspase-3, PARP, and GAPDH were analyzed. Intact caspase-3 and PARP are labeled, and cleaved portions are indicated by the arrow (cleaved caspase-3: −17 kDa, cleaved PARP: −85 kDa). Numbers 1–10 along the bottom of images represent lane numbers. Blots are representative of three independent experiments. (**b**) Myoblasts were pretreated with 10 μM Akti (upper left panel), 10 μM U0126 (upper right panel), or Akti and U0126 (lower panel) for 1–h, as indicated. Following the pre-incubation period, cells were treated with 125 ng/ml IGF-I for 30–min before addition of 400 μM H$_2$O$_2$ as indicated. Western blotting was performed as described in panel **b**. Representative blots of two independent experiments for each condition are shown

Akt kinase assay. Immune complex kinase assays were performed by a protocol of an assay kit purchased from Cell Signaling Technologies. Cell lysates (200 μg) were incubated with anti-Akt1, anti-Akt2, or anti-Akt3 antibody overnight at 4°C in cell lysis buffer. Immune complexes were then rotated for 2–4 h at 4°C with protein A-conjugated agarose beads (20 μl of 50% slurry/reaction) before being washed twice in cell lysis buffer and twice in kinase buffer (25 mM Tris-HCl (pH 7.5), 5 mM β-glycerophosphate, 2 mM dithiothreitol, 0.1 mM Na$_3$VO$_4$, 10 mM MgCl$_2$). After resuspension in kinase assay buffer containing ATP and a GST–GSK-3α/β fusion protein (residues surrounding GSK-3α/β Ser 21/9 (CGPKGPGRRGRRR TSSFAEG)), the reaction was allowed to proceed at 30°C for 30 min. After the reaction was stopped by addition of concentrated SDS-PAGE loading buffer,

samples were separated by SDS-PAGE and transferred to PVDF membranes as described above. Immunoblotting was performed using primary antibodies to phospho-GSK-3α/β provided in the kinase assay kit, followed by addition of HRP-conjugated secondary antibodies, detection by ECL, and exposure to X-ray film. Results were quantitated by densitometry.

Cell-surface receptor. Analysis of IGF-IR at the cell surface was accomplished by using a commercially available cell-surface protein isolation kit (Pierce, Rockford, IL, USA). Briefly, for each treatment, four 100-mm culture dishes were seeded with C2C12 cells and transfected as described above. Cells were labeled with sulfo-NHS-SS-biotin for 30 min and the reaction quenched with the
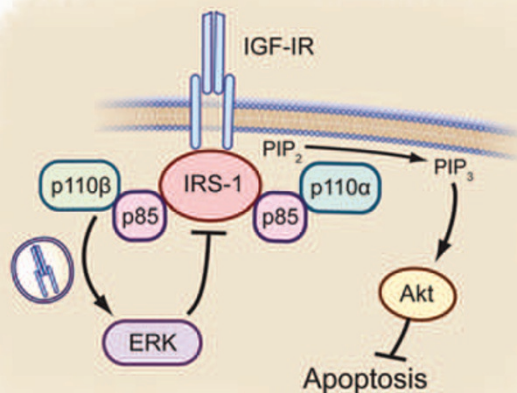
Figure 7 Proposed mechanism of IGF-I signal transduction in myoblasts. Signaling through IGF-IR recruits adaptor molecules including IRS-1 to IGF-IR. This promotes binding of PI3K and generation of 3′ lipid phosphoinositides that recruit other molecules, including Akt, to the membrane, ultimately resulting in their activation. PI3K p110α catalytic subunit is required for Akt activation, but p110β is not. A second pathway includes non-catalytic action of p110β that is associated with IGF-IR internalization and is required for activation of ERK. ERK may then phosphorylate IRS-1 at Ser 636/639, inhibiting PI3K binding and promoting IRS-1 degradation, thus attenuating IGF-IR signals

provided quenching solution. Cells were transferred to 50-ml conical tubes, centrifuged, and washed with TBS. Lysis buffer provided in the kit was added to cell pellets and transferred to microfuged tubes and briefly sonicated every 10 min for 30 min at a power of 1.5 followed by clarification of supernatant, which was quantified and 1.4 g added to provided spin columns. At this point, some protein lysate was stored at −80°C for analysis of total IGF-IR or GAPDH. Biotin-labeled proteins were washed and isolated with NeutrAvidin Agarose (provided in the kit) with end-over-end mixing for 1 h. Agarose/biotinylated complexes were washed and incubated in sample buffer (62.5 mM Tris (pH 6.8), 2% SDS, 20% glycerol) for 1 h, centrifuged, and the eluate was collected. A small amount of bromophenol blue was added to eluate and proteins were separated by SDS-PAGE followed by western blotting for IGF-IR or GAPDH as described above.

Detection of PI(3,4,5)P3. Levels of PI(3,4,5)P3 were determined by using a commercially available ELISA assay (Echelon Biosciences, Salt Lake City, UT, USA; P/N K-1000) following the manufacturer's instructions. Briefly, after treatment, cells were washed three times in Buffer A (20 mM Tris-HCl (pH 7.4), 137 mM NaCl, 1 mM CaCl$_2$, 1 mM MgCl$_2$, and 0.1 mM sodium orthovanadate) and incubated at 4°C for 30 min in Buffer A plus 1% NP-40 and 1 mM PMSF. Insoluble material was removed by centrifugation and clarified lysates quantified. A 125-μg weight was immuno-precipitated with either p110α or p110β antibody for 2 hours at 4°C, followed by mixing with Protein-A/G agarose beads (Santa Cruz) for 1 h. Immunocomplexes were washed three times with Buffer A plus 1% NP-40, three times with 0.1 M Tris-HCl (pH 7.4); 5 mM LiCl, and 0.1 mM sodium orthovanadate, and twice in TNE (10 mM Tris-HCl (pH 7.4), 150 mM NaCl, 5 mM EDTA, and 0.1 mM sodium orthovanadate). Kinase reactions were performed in triplicate by incubation in PI3K reaction buffer (20 mM Tris (pH 7.4), 10 mM NaCl, 4 mM MgCl$_2$, and 25 μM ATP) and 100 μM PI(4,5)P2 substrate for 2 h, followed by centrifugation to stop the reactions and addition of PI(3,4,5)P3 detector for 1 hour. At this time, PIP3 standards (provided) were set up using concentrations of 200, 100, 50, 25, 12.5, and no lipid control. Reacted mixtures and standards were then transferred to the detection plate for 60 min, washed once in TBS-T, and secondary detector added for 30 min. Wells were washed three times with TBS-T and then 100 μl of TMB solution added to induce color change. Color development was stopped by addition of 1 N H$_2$SO$_4$ stop solution when color development was within the linear range of standards, followed by reading at 450 nm.

Statistics. Data are presented as means ± S.E.M. Statistics were performed using either one-way or two-way ANOVA and multiple range tests *a posteriori*,

as described in the figure legends. Densiometric analysis was performed using Image J 1.60 (http://rsbweb.nih.gov/ij/). A *P*-value < 0.05 was considered significant.

1. Vanhaesebroeck B, Waterfield MD. Signaling by distinct classes of phosphoinositide 3-kinases. *Exp Cell Res* 1999; **253**: 239–254.
2. Hirsch E, Costa C, Ciraolo E. Phosphoinositide 3-kinases as a common platform for multi-hormone signaling. *J Endocrinol* 2007; **194**: 243–256.
3. Geering B, Cutillas PR, Nock G, Gharbi SI, Vanhaesebroeck B. Class IA phosphoinositide 3-kinases are obligate p85–p110 heterodimers. *Proc Natl Acad Sci USA* 2007; **104**: 7809–7814.
4. Denley A, Kang S, Karst U, Vogt PK. Oncogenic signaling of class I PI3K isoforms. *Oncogene* 2008; **27**: 2561–2574.
5. Kang S, Denley A, Vanhaesebroeck B, Vogt PK. Oncogenic transformation induced by the p110beta, -gamma, and -delta isoforms of class I phosphoinositide 3-kinase. *Proc Natl Acad Sci USA* 2006; **103**: 1289–1294.
6. Samuels Y, Wang Z, Bardelli A, Silliman N, Ptak J, Szabo S *et al*. High frequency of mutations of the PIK3CA gene in human cancers. *Science* 2004; **304**: 554.
7. Vogt PK, Gymnopoulos M, Hart JR. PI 3-kinase and cancer: changing accents. *Curr Opin Genet Dev* 2009; **19**: 12–17.
8. Chaussade C, Rewcastle GW, Kendall JD, Denny WA, Cho K, Gronning LM *et al*. Evidence for functional redundancy of class IA PI3K isoforms in insulin signalling. *Biochem J* 2007; **404**: 449–458.
9. Papakonstanti EA, Zwaenepoel O, Bilancio A, Burns E, Nock GE, Houseman B *et al*. Distinct roles of class IA PI3K isoforms in primary and immortalised macrophages. *J Cell Sci* 2008; **121** (Pt 24): 4124–4133.
10. Knight ZA, Gonzalez B, Feldman ME, Zunder ER, Goldenberg DD, Williams O *et al*. A pharmacological map of the PI3-K family defines a role for p110alpha in insulin signaling. *Cell* 2006; **125**: 733–747.
11. Foukas LC, Claret M, Pearce W, Okkenhaug K, Meek S, Peskett E *et al*. Critical role for the p110alpha phosphoinositide-3-OH kinase in growth and metabolic regulation. *Nature* 2006; **441**: 366–370.
12. Guillermet-Guibert J, Bjorklof K, Salpekar A, Gonella C, Ramadani F, Bilancio A *et al*. The p110beta isoform of phosphoinositide 3-kinase signals downstream of G protein-coupled receptors and is functionally redundant with p110gamma. *Proc Natl Acad Sci USA* 2008; **105**: 8292–8297.
13. Jia S, Liu Z, Zhang S, Liu P, Zhang L, Lee SH *et al*. Essential roles of PI(3)K-p110beta in cell growth, metabolism and tumorigenesis. *Nature* 2008; **454**: 776–779.
14. Bi L, Okabe I, Bernard DJ, Nussbaum RL. Early embryonic lethality in mice deficient in the p110beta catalytic subunit of PI 3-kinase. *Mamm Genome* 2002; **13**: 169–172.
15. Marques M, Kumar A, Poveda AM, Zuluaga S, Hernandez C, Jackson S *et al*. Specific function of phosphoinositide 3-kinase beta in the control of DNA replication. *Proc Natl Acad Sci USA* 2009; **106**: 7525–7530.
16. Ciraolo E, Iezzi M, Marone R, Marengo S, Curcio C, Costa C *et al*. Phosphoinositide 3-kinase p110beta activity: key role in metabolism and mammary gland cancer but not development. *Sci Signal* 2008; **1** ra3.
17. Brachmann SM, Ueki K, Engelman JA, Kahn RC, Cantley LC. Phosphoinositide 3-kinase catalytic subunit deletion and regulatory subunit deletion have opposite effects on insulin sensitivity in mice. *Mol Cell Biol* 2005; **25**: 1596–1607.
18. Jones JI, Clemmons DR. Insulin-like growth factors and their binding proteins: biological actions. *Endocr Rev* 1995; **16**: 3–34.
19. Kooijman R. Regulation of apoptosis by insulin-like growth factor (IGF)-I. *Cytokine Growth Factor Rev* 2006; **17**: 305–323.
20. Peruzzi F, Prisco M, Dews M, Salomoni P, Grassilli E, Romano G *et al*. Multiple signaling pathways of the insulin-like growth factor 1 receptor in protection from apoptosis. *Mol Cell Biol* 1999; **19**: 7203–7215.
21. Lawlor MA, Rotwein P. Coordinate control of muscle cell survival by distinct insulin-like growth factor activated signaling pathways. *J Cell Biol* 2000; **151**: 1131–1140.
22. Hong F, Kwon SJ, Jhun BS, Kim SS, Ha J, Kim SJ *et al*. Insulin-like growth factor-1 protects H9c2 cardiac myoblasts from oxidative stress-induced apoptosis via phosphatidylinositol 3-kinase and extracellular signal-regulated kinase pathways. *Life Sci* 2001; **68**: 1095–1105.
23. Baregamian N, Song J, Jeschke MG, Evers BM, Chung DH. IGF-1 protects intestinal epithelial cells from oxidative stress-induced apoptosis. *J Surg Res* 2006; **136**: 31–37.
24. Oliver FJ, de la Rubia G, Rolli V, Ruiz-Ruiz MC, de Murcia G, Murcia JM. Importance of poly(ADP-ribose) polymerase and its cleavage in apoptosis. Lesson from an uncleavable mutant. *J Biol Chem* 1998; **273**: 33533–33539.
25. Franke TF, Kaplan DR, Cantley LC, Toker A. Direct regulation of the Akt proto-oncogene product by phosphatidylinositol-3,4-bisphosphate. *Science* 1997; **275**: 665–668.

26. Bouzakri K, Roques M, Gual P, Espinosa S, Guebre-Egziabher F, Riou JP et al. Reduced activation of phosphatidylinositol-3 kinase and increased serine 636 phosphorylation of insulin receptor substrate-1 in primary culture of skeletal muscle cells from patients with type 2 diabetes. *Diabetes* 2003; **52**: 1319–1325.

27. Hayakawa M, Kaizawa H, Moritomo H, Koizumi T, Ohishi T, Okada M et al. Synthesis and biological evaluation of 4-morpholino-2-phenylquinazolines and related derivatives as novel PI3 kinase p110alpha inhibitors. *Bioorg Med Chem* 2006; **14**: 6847–6858.

28. Barnett SF, Defeo-Jones D, Fu S, Hancock PJ, Haskell KM, Jones RE et al. Identification and characterization of pleckstrin-homology-domain-dependent and isoenzyme-specific Akt inhibitors. *Biochem J* 2005; **385** (Pt 2): 399–408.

29. Jia S, Roberts TM, Zhao JJ. Should individual PI3 kinase isoforms be targeted in cancer? *Curr Opin Cell Biol* 2009; **21**: 199–208; e-pub 2009 Feb 4.

30. Mothe I, Van Obberghen E. Phosphorylation of insulin receptor substrate-1 on multiple serine residues, 612, 632, 662, and 731, modulates insulin action. *J Biol Chem* 1996; **271**: 11222–11227.

31. Brognard J, Sierecki E, Gao T, Newton AC. PHLPP and a second isoform, PHLPP2, differentially attenuate the amplitude of Akt signaling by regulating distinct Akt isoforms. *Mol Cell* 2007; **25**: 917–931.

32. Gao T, Furnari F, Newton AC. PHLPP: a phosphatase that directly dephosphorylates Akt, promotes apoptosis, and suppresses tumor growth. *Mol Cell* 2005; **18**: 13–24.

33. Chow JC, Condorelli G, Smith RJ. Insulin-like growth factor-I receptor internalization regulates signaling via the Shc/mitogen-activated protein kinase pathway, but not the insulin receptor substrate-1 pathway. *J Biol Chem* 1998; **273**: 4672–4680.

34. Kim AH, Khursigara G, Sun X, Franke TF, Chao MV. Akt phosphorylates and negatively regulates apoptosis signal-regulating kinase 1. *Mol Cell Biol* 2001; **21**: 893–901.

35. Datta SR, Dudek H, Tao X, Masters S, Fu H, Gotoh Y et al. Akt phosphorylation of BAD couples survival signals to the cell-intrinsic death machinery. *Cell* 1997; **91**: 231–241.

36. Brunet A, Bonni A, Zigmond MJ, Lin MZ, Juo P, Hu LS et al. Akt promotes cell survival by phosphorylating and inhibiting a Forkhead transcription factor. *Cell* 1999; **96**: 857–868.

37. Brunet A, Park J, Tran H, Hu LS, Hemmings BA, Greenberg ME. Protein kinase SGK mediates survival signals by phosphorylating the forkhead transcription factor FKHRL1 (FOXO3a). *Mol Cell Biol* 2001; **21**: 952–965.

38. Bradford MM. A rapid and sensitive method for the quantitation of microgram quantities of protein utilizing the principle of protein-dye binding. *Anal Biochem* 1976; **72**: 248–254.